Hermosilla, T.; Coops, N.; Ruiz Fernández, LÁ.; Moskal, M. (2014). Deriving pseudo-vertical waveforms from small-footprint full-waveform LiDAR data. Remote Sensing Letters. 5(4):332-341. doi:10.1080/2150704X.2014.903350.

# Deriving pseudo-vertical waveforms from small-footprint full-waveform LiDAR data

T. Hermosilla*[ab], N.C. Coops[a], L.A. Ruiz[b], and L.M. Moskal[c]

[a]*Integrated Remote Sensing Studio, University of British Columbia, BC, Canada.*

[b]*Geo-Environmental Cartography and Remote Sensing Group (CGAT), Universitat Politècnica de València, Spain.*

[c]*Remote Sensing and Geospatial Analysis Laboratory, Precision Forestry Cooperative, School of Environmental and Forest Sciences, University of Washington, WA, USA.*

Corresponding author. Email: txomin.hermosilla@live.forestry.ubc.ca

Integrated Remote Sensing Studio, Department of Forest Resources Management, University of British Columbia, Vancouver, BC, V6T 1Z4, Canada.

# Deriving pseudo-vertical waveforms from small-footprint full-waveform LiDAR data

When processing scanning LiDAR data, it is commonly assumed that the extracted full-waveform LiDAR pulse registers truly vertical information of forest canopies. This assumption may lead to uncertain results for the spatio-temporal analysis of the waveforms due to off-nadir scanning angles and various trajectories traveled by the pulses in overlapping strips. In this letter we investigate these assumptions, and undertake some preliminary analysis to overcome their impacts on forest-based LiDAR analyses. Our results demonstrate that for a standard LiDAR forest acquisition program in Oregon, USA, most of the hits (83%) are acquired off-nadir, which leads to positional displacements on the ground of the full-waveforms of about 0.20 m for each one-meter height increment. We propose an approach to synthetize multiple waveform data into composite waveforms containing the vertical profile of vegetation for a given location. This approach is based on partitioning the aboveground vertical space into voxels and using the maximum full-waveform intensity value to construct new full-waveforms comprising the vertical information of the various waveforms crossing over a location. Our initial results indicate that deriving spatio-temporal metrics from the composite pseudo-vertical full-waveforms produces a more consistent response across adjacent height levels, which in turn enables a more complete characterization and more vegetation structure to be retrieved. We conclude that this type of pseudo-vertical full-waveform analysis is necessary to more fully understand the impact of the return signals from tree crowns.

Keywords: Airborne laser scanner; forestry; full-waveform LiDAR.

Subject classification codes: include these here if the journal requires them

## 1. Introduction

LiDAR (Light Detection And Ranging) technology has experienced a significant increase in application within the forestry community and is routinely used to estimate a range of structural parameters for forest inventory in a number of countries and jurisdictions (van Leeuwen and M. Nieuwenhuis 2010). To date, the most common type

of LiDAR data acquired is discrete return data where the return pulse is digitized into a small number of discrete three-dimensional coordinates, usually coinciding with the return of the first and last energy components and some intermediate energy peaks (Hall et al. 2005).

Recently, small-footprint full-waveform LiDAR sensors have been developed which have the potential to provide new opportunities for vegetation studies (Mallet and Bretar 2009; Allouis et al. 2012). Full-waveform sensors register the complete returned backscattered signal, and analysis of the full-waveform should enable researchers to describe, more fully, the physical properties of the intercepted objects. The amplitude of the waveform at any height is proportional to the amplitude of the energy received at that given height, the amount of reflective material intercepted, the orientation of that material, and its reflectance (Hyde et al. 2005). The use of full-waveform data is increasing in some forestry applications, such as single tree detection (Reitberger et al. 2009; Yao, Krzystek and Heurich 2012), dead tree identification (Mücke, Hollaus and Pfeifer 2012), tree species classification (Reitberger, Krzystek and Stilla 2008; Neuenschwander, Magruder and Tyler 2012; Heinzel and Koch 2011; Sarrazin et al. 2012; Neuenschwander 2012; GuangCai 2012), and forest structural variables estimation (Koetz et al. 2006; Wu et al. 2009; Kim et al. 2009; Ferraz et al. 2012; Kronseder et al. 2012; Sumnall, Hill and Hinsley 2012).

Although commercial small-footprint full-waveform systems are relatively new, large-footprint full-waveform LiDAR data have been available in the past two decades. One of the earliest large-footprint airborne full-waveforms sensors was SLICER (Scanning LiDAR Imager of Canopies by Echo Recovery, 10 m footprint) and more recently LVIS (Laser Vegetation Imaging Sensor, 25 m footprint) both of which have been applied to vegetation studies worldwide (Hyde et al. 2005; Lefsky et al. 1999; Ni-

Meister, Jupp and Dubayah 2001; Blair, Rabine and Hofton 1999; Drake 2002). Moreover, since 2003 GLAS (Geoscience Laser Altimeter System) sensor, carried by ICESat satellite, provides waveform data from space with 70 m footprint. In addition to successful application to estimate various parameters, such as vegetation vertical structure (Harding and Carabajal 2005) or biomass predictions (Boudreau et al 2006; Peterson, Nelson and Wylie 2012), a number of studies have used this data to validate spaceborne and airborne data products (Sun et al. 2008).

Compared to discrete return LiDAR datasets, full-waveforms provide large amounts of data about the forest canopy. To date, two approaches for processing full-waveforms have emerged (Mallet and Bretar 2009). Signal decomposition and pulse detection methods can be used to extract a large number of echoes from the waveforms themselves, and therefore create very dense point clouds. Standard techniques can be applied to these point clouds similar to those used for discrete LiDAR data, such as height and cover metrics, height percentiles, and others derived from canopy height models. A second approach, which has received less attention, is based on a spatio-temporal analysis of the return waveform, to extract detailed geometric and radiometric information. Previously, this type of approach was developed for SLICER, LVIS and GLAS and provides metrics such as Height of Median Energy (HOME), peak distances, canopy roughness, waveform energy, etc. (Drake et al 2002; Carabajal and Harding 2005; Duong 2010). To date, some researchers have adapted these spatio-temporal approaches to small-footprint data in order to incorporate or complete these descriptors for individual waveform analysis (Neuenschwander, Magruder and Tyler 2009; Heinzel and Koch 2011; Sarrazin et al. 2012; Neuenschwander 2012; GuangCai et al. 2012; Höfle, Hollaus and Hagenauer 2012).

While spaceborne sensors (GLAS) have a small off-nadir pointing angle (Bretar, Pierrot-Deseilligny and Roux 2004) and SLICER has near-nadir viewing, most full-waveforms acquired by LVIS or small-footprint sensors are off-nadir. The closer the pulses are located to the edge of the swath width, the greater the acquisition scanning angle, and therefore the more oblique path travelled by the pulse. The effect of off-nadir pointing has been analyzed from both large footprint observations (Neuenschwander 2008; Yang, Ni-Meister and Lee 2011) and simulated data (Pang et al. 2011) with results indicating that the waveform is stretched as off-nadir angle increases. As airborne LiDAR acquisition is generally composed by many overlapping strips (Bretar, Pierrot-Deseilligny and Roux 2004), waveforms for specific locations may have been recorded from several flight trajectories. Consequently, the various waveforms representing specific three-dimensional locations within a canopy would have traveled different paths and, hence, crossed different canopy elements prior to intersection. These different transition paths may be especially problematic when summarizing information on forest canopies due to the large number of intercepted objects, the high density of LiDAR data, and the limited penetration power of the laser pulse. If not correctly accounted for, the false assumption that waveforms register vertical information on the forest canopy may lead to ambiguous outcomes for a same location.

In order to avoid relying on assumptions of vertical waveforms across the entire scan swath and integrating non-vertical waveforms from different flight trajectories, we propose an approach that allows multiple waveform data to be synthesized into composite waveforms representing the correct vertical profile of vegetation for a given location. The proposed approach utilizes voxels to partition the vertical space around the canopy using the maximum full-waveform recorded intensity value to construct new waveforms comprising the vertical information of the various waveforms crossing over

a location. This approach is divided into four steps: de-noising and smoothing, spatial location and normalized height calculation, space partitioning by means of voxels, and pseudo-vertical full-waveform construction. With this voxel-based model of LiDAR pulses, we expect a more realistic and accurate representation of the pulse's vertical transmission to correct the off-nadir effect. Therefore it is a more appropriate approach for modeling a range of forest structural attributes.

In this letter we will: (i) examine the proportion of off-nadir pulses and compute the positional error associated with those non-vertical hits; (ii) propose a new approach to derive pseudo-vertical full-waveforms; and (iii) compare and contrast the behavior of spatio-temporal metrics computed from pseudo-vertical waveforms and from observed waveforms.

## 2. Study Area and Data

Data acquired for this research came from the Panther Creek Cooperative Research Project (Flewelling and McFadden 2011), which is intended to develop a suite of LiDAR applications for forest managers and currently involves over forty researchers and land managers representing federal, state and local agencies, landowners, a LiDAR provider, universities, and consultants.

The Panther Creek study area is a 2,258 ha forested area located in the east side of the coastal mountain range in Oregon, USA, with an elevation ranging from 100 to 700 m. The dominant species is Douglas fir, offering within half of the stands with the reminder mixed with other conifers (western hemlock, western cedar and grand fir), or deciduous species (red alder and bigleaf maple). Average tree height is 40 m. Full-waveform LiDAR data were acquired on July 15 2010 by Watershed Sciences, Inc. for the United States Bureau of Land Management (USBLM) using a Leica ALS60 sensor mounted in a Cessna Caravan 208B. The system acquired data at 105 kHz pulse rate,

flown at 900 meters above ground level, with a scanning angle of ±14º from nadir, a waveform temporal sample spacing of 2 ns and a footprint size of 0.25 m. This configuration yielded a nominal pulse density of ≥8 points/m2. The study area was surveyed with opposing flight line side-lap of ≥50% (≥100% overlap) to reduce laser shadowing and increase laser coverage. LiDAR data were distributed in LAS 1.3 format. In addition to the full-waveform data, a Digital Terrain Model (DTM) was provided by Watershed Sciences, Inc. based on last return pulses acquired within this LIDAR mission with a documented Root-Mean-Square Error using 33 GPS ground control points of 0.19 m.

## 3. Method

### *3.1. Determination of the off-nadir full-waveforms*

To determine the number of off-nadir full-waveforms for a given forest stand, the scanning angle for each hit is required. This information is recorded within the LAS 1.3 files which also contain the discrete return positions, their associated full-waveform, the return point location within the waveform, and the parameters defining a parametric line equation to extrapolate points along the associated waveforms (see ASPRS 2010). The "scan angle rank" value recorded in the LAS file however is rounded to an integer making it imprecise for our analysis. For this reason, the parametric line equation was used to provide additional information on the three dimensional spatial displacement for each waveform record. This information and trigonometric equations (Baltsavias 1999) were then used to retrieve a more precise scanning angle for each pulse without any rounding or ranking.

### *3.2. Spatio-temporal metrics derived from full-waveforms*

A set of spatio-temporal metrics characterizing the return full-waveform was used to estimate the variability introduced into the analysis of the observed waveforms on the assumption they were acquired vertically. The following metrics were calculated to assess the effect of considering the observed full-waveforms as vertical: HOME, roughness of outermost canopy, number of peaks, and return waveform energy. Several of these metrics were initially developed using large-footprint waveform sensors. However, the use of the metrics at finer scales provided by small-footprint data has been shown to be successful, and most of the variables can readily be used to describe within crown – rather than within stand canopy – variations (Neuenschwander, Magruder and Tyler 2009; Heinzel and Koch 2011; Neuenschwander 2012; GuangCai et al. 2012; Höfle, Hollaus and Hagenauer 2012). HOME represents the height associated to median energy location, and it is computed as the distance from the ground (defined by the DTM) to the position were the return energy is divided into two equal parts. The roughness of outermost canopy is defined as the distance from the waveform beginning to the first peak, usually considered as the peak of canopy. The number of peaks is derived from a peak detection process, and it describes the number of height levels crossed by the waveform. The return waveform energy represents the total received energy aboveground.

### *3.3. Construction of pseudo-vertical full-waveforms*

To date, a small number of studies have proposed combining several non-vertical waveforms to retrieve fully vertical information. Allouis et al. (2012) computed cumulative waveforms from the sum of full-waveforms signals falling within a tree-crown boundary. Wu et al. (2012) proposed an angular rectification based on the interpolation of waveform record intensity values, whereas Buddenbaum, Seeling and

Hill (2013) used the mean intensity value. These approaches, however, may mask or blur the information of most significant peaks of waveforms by averaging or mixing them with other less relevant intensity values. To reduce this unwanted diffusion of the height and intensity our approach has four key steps: de-noising and smoothing, spatial location and normalized height calculation, space partitioning by means of voxels, and pseudo-vertical full-waveform construction.

i) An initial noise assessment was performed to distinguish between noise and actual signal by establishing a threshold determined as the mean plus four times the standard deviation (Duong 2010). After removing noisy waveforms, the background noise of each full-waveform was suppressed. Full-waveforms were then smoothed and any remaining noise removed using a Gaussian filter, with a kernel size defined by the Full Width at Half Maximum.

ii) Each full-waveform record was spatially located using the information contained in LAS files. Each waveform record was normalized by computing the difference between their height and the DTM, discarding from the analysis those records located belowground.

iii) Next, vertical canopy space was partitioned in regular voxels. To produce waveforms with analogous dimensions than the originals, 0.25 × 0.25 × 0.30 m voxels were created, approximately corresponding to the footprint size and the distance traveled by the pulse during the temporal sample spacing of the full-waveform. Each voxel was filled with the maximum amplitude value of waveform records within it. The maximum was used to preserve in the composited waveforms the significance of the major returns of the observed waveforms. As Figure 1 shows, the returned intensity of the waveforms acquired at off-nadir angles is slightly lower than those acquired from angles closer to nadir. For angles less than or equal to 7°, the gain reduction is less than

1%, while the reduction for larger angles is lower than 3%. This implies that the scanning angle has a minor effect on the returned intensity. Still, by assigning the maximum value to characterize the pseudo-vertical waveform, our approach favors near-nadir scan angles in place of off-nadir returns.

iv) Lastly, the pseudo-vertical full-waveforms were constructed by extracting the information contained in the vertical voxels over a specific location.

## 4. Results

The frequency distribution of hits and scanning angle for an actual LiDAR strip is shown in Figure 2. As expected, near-nadir hits (acquired with a scanning angle < 3°) accounted for only 17% of the total acquired pulses. As a result, 83% of pulses were non-nadir, with 22% > 12° (Figure 2). The relationship between scanning angle from nadir and the positional displacement on the ground computed at vertical 1 m increments is shown in Figure 3. The figure indicates that, at nadir, the maximum positional displacement for each 1 m height increment is < 0.05 m, whereas at a maximum scanning angle this horizontal displacement (computed as defined by Baltsavias 1999) can be as large as 0.20 m. Given an average tree height of 40 m in our study area, this results in a maximum horizontal displacement in excess of 8 m, and greater than 10 m for the largest scanning angle values registered (14°).

The results of the pseudo-vertical full-waveform voxels approach for a specific voxel column (a) and the observed non-vertical waveforms associated with this same vertical location are shown in Figure 4. As the figure shows multiple waveforms intersect this column of 3D voxels, with none providing a comprehensive description of the vertical structure. A number of the waveforms have peaks in intensity around 40 m height (Figure 4.b, Figure 4.c, Figure 4.d,), whereas other waveforms (Figure 4.e, Figure 4.f) have their major peaks at heights between 15 and 20 m. There is a third

group for waveforms distributed at a range of heights that only show minor interaction (Figure 4.g, Figure 4.h). Since the pseudo-vertical full-waveforms are composed by the maximum intensity information of all the observed waveforms crossing a vertical space, independent of the spatial location of the hits, several of these peaks may not be represented by the composite full-waveform characterizing a specific vertical location.

Differences between the individual non-vertical pulses within the same column of voxels are also evident when we examine a range of spatio-temporal metrics computed from each waveform (see Table 1). Results indicate that, while some metrics (return waveform energy and HOME) are relatively consistent across all of the intersecting waveforms (coefficient of variation ranging from 25 to 33%), some others, such as VDR and the number of peaks, produce very high coefficient of variation values (ranging from 70 to 109%). These very large values results demonstrate that the assumption of vertical waveforms can produce highly variable outcomes due to differences in scanning angle with the waveforms which in fact are traveling along very different flight trajectories, intersecting a range of stand structure.

Figure 5 shows the behavior of various spatio-temporal metrics (HOME, return waveform energy, number of peaks, and roughness of outermost canopy) for an example plot computed from the observed (above) and the pseudo-vertical (bellow) full-waveforms with 0.25 m pixel size. The metrics for the observed waveforms are located according to the coordinates of their anchor point. Assuming multiple anchor points in the vertical space associated with the same location, the average metric value of all related waveforms is used to characterize that location. The use of composite pseudo-vertical full-waveforms characterizes the vertical structure of each location with a single waveform, avoiding situations where several waveforms are related to a same location. The results show that pseudo-vertical full-waveforms provide a denser and more

continuous coverage, resulting in fewer null pixels when compared to the observed waveforms. The spatio-temporal metrics computed from the pseudo-vertical full-waveforms show an enhanced characterization of vegetation, allowing more structure to be retrieved and producing a more consistent response at adjacent height levels. In addition, there is an increased variability in the metrics across the observed land cover types (forest, other vegetation and bare soil). This potentially facilitates increased discrimination among different land covers and vegetation types.

## 5. Conclusions

The use of three dimensional voxel space for representing full-waveform LiDAR data provides an alternative to the direct analysis of observed full-waveforms which are mostly collected from off-nadir angles. The proposed pseudo-vertical full-waveforms condense and summarize the main returned energy information of the several observed full-waveforms crossing the vertical space of a location, with analogous temporal sample spacing and footprint dimensions. In contrast to the direct analysis of observed full-waveforms, peaks and energy distribution of composite waveforms are related with the actual vertical space of a specific location. Results suggest that considering pseudo-vertical full-waveforms to derive spatio-temporal metrics instead of observed waveforms may lead to an enhanced description of the vegetation structure, producing a denser full-waveform coverage. The results presented in this letter are a result of preliminary analysis and suggest that additional research should be undertaken as analysis of small-footprint, full-waveform LiDAR data becomes more commonplace in forestry applications. These investigations could include a more exhaustive validation of the model using field data, and to more comprehensively model the effect of the variation of returned intensity due to changes in altitude, which may hinder the retrieval of some returns.

**Acknowledgements**

This paper was developed as a result of a visiting scholar grant funded by the Erasmus Mundus Programme of the European Commission under the Transatlantic Partnership for Excellence in Engineering - TEE Project. The authors also wish to thank also the Generalitat Valenciana for the mobility grant BEST/2012/235, and the Panther Creek Remote Sensing and Research cooperative program for the data provided for this research.

**References**

Allouis, T., S. Durrieu, C. Véga, and P. Couteron. 2012. "Stem volume and above-ground biomass estimation of individual pine trees from LiDAR data: contribution of full-waveform signals." IEEE Journal of Selected Topics in Applied Earth Observations and Remote Sensing 6 (2): 924-934.

Baltsavias, E.P. 1999. "Airborne laser scanning: basic relations and formulas." ISPRS Journal of Photogrammetry and Remote Sensing 54 (2): 199-214.

Blair, J.B., D. L. Rabine, and M. A. Hofton. 1999. "The laser vegetation imaging sensor: a medium-altitude, digitisation-only, airborne laser altimeter for mapping vegetation and topography." ISPRS Journal of Photogrammetry and Remote Sensing 54 (2): 115-122.

Boudreau, J., R. F. Nelson, H. A. Margolis, A. Beaudoin, L. Guindon, and D. S. Kimes. 2008. "Regional aboveground forest biomass using airborne and spaceborne LiDAR in Québec." Remote Sensing of the Environment 112 (10): 3876-3890.

Bretar, F., M. Pierrot-Deseilligny, and M. Roux. 2004. "Solving the strip adjustment problem of 3D airborne lidar data." IEEE International Geoscience and Remote Sensing Symposium Proceedings, Anchorage, AK, 4734-4737.

Buddenbaum, K., S. Seeling, and J. Hill. 2013. “Fusion of full-waveform lidar and imaging spectroscopy remote sensing data for the characterization of forest stands.” International Journal of Remote Sensing 34 (13): 4511-4524.

Carabajal, C.C., and D. J. Harding. 2005. “ICESat validation of SRTM C-band digital elevation models.” Geophysical Research Letters 32 (22): L22S01.

Drake, J.B., R. O. Dubayah, D. B. Clark, R. G. Knox, J. B. Blair, M. A. Hofton, R. L. Chazdon, J. F. Weishampel, and S. Prince. 2002. “Estimation of tropical forest structural characteristics using large-footprint lidar.” Remote Sensing of the Environment 79 (2): 305-319.

Duong, H.V. 2010. “Processing and application of icesat large footprint full waveform laser range data.” Ph.D dissertation. Delft University of Technology, Netherlands.

Ferraz, A., G. Goncalves, P. Soares, M. Tome, C. Mallet, S. Jacquemoud, F. Bretar, and L. Pereira. 2012. “Comparing small-footprint lidar and forest inventory data for single strata biomass estimation - a case study over a multi-layered Mediterranean forest.” IEEE Geoscience and Remote Sensing Symposium (IGARSS). 6384-6387.

Flewelling, J.W., and G. McFadden. 2011. “Lidar Data and Cooperative Research at Panther Creek, Oregon.” Paper presented at Silvilaser 2011, the 11th International Conference on Lidar Applications for Assessing Forest Ecosystems, Hobart, Australia, October 16-19.

GuangCai, X., P. Yong, L. Zengyuana, Z. Dan, and L. Luxia. 2012. “Individual trees species classification using relative calibrated full-waveform LiDAR data.” Paper presented at SilviLaser 2012, the 12th International Conference on Lidar Applications for Assessing Forest Ecosystems, Vancouver, BC, September 16-19.

Hall, S. A., I. C. Burke, D. O. Box, M. R. Kaufmann, and J. M. Stoker. 2005. "Estimating stand structure using discrete-return lidar: an example from low density, fire prone ponderosa pine forests." Forest Ecology and Management 208 (1): 189-209.

Harding, D.J., and C. C. Carabajal. 2005. "ICESat waveform measurements of within-footprint topographic relief and vegetation vertical structure." Geophysical Research Letters 32 (21): L21S10.

Heinzel, J., and B. Koch. 2011. "Exploring full-waveform LiDAR parameters for tree species classification." International Journal of Applied Earth Observation and Geoinformation 13 (1): 152-160.

Höfle, B., M. Hollaus, and J. Hagenauer. 2012. "Urban vegetation detection using radiometrically calibrated small-footprint full-waveform airborne LiDAR data." ISPRS Journal of Photogrammetry and Remote Sensing 67: 134-147.

Hyde, P., R. Dubayah, B. Peterson, J. B. Blair, M. Hofton, C. Hunsaker, and W. Walker. 2005. "Mapping forest structure for wildlife habitat analysis using waveform lidar: validation of montane ecosystems." Remote Sensing of Environment 96 (3): 427-437.

Kim, Y., Z. Yang, W. B. Cohen, D. Pflugmacher, C. L. Lauver, and J. L. Vankat. 2009. "Distinguishing between live and dead standing tree biomass on the North Rim of Grand Canyon National Park, USA using small-footprint lidar data," Remote Sensing of the Environment 113 (11): 2499-2510.

Koetz, B., F. Morsdorf, G. Sun, K. J. Ranson, K. Itten, and B. Allgower. 2006. "Inversion of a lidar waveform model for forest biophysical parameter estimation." IEEE Geoscience and Remote Sensing 3 (1): 49-53.

Kronseder, K., U. Ballhorn, V. Böhm, and F. Siegert. 2012. "Above ground biomass estimation across forest types at different degradation levels in Central Kalimantan

using LiDAR data." International Journal of Applied Earth Observation and Geoinformation 18: 37-48.

Lefsky, M.A., W. B. Cohen, S. A. Acker, G. G. Parker, T. A. Spies, and D. Harding. 1999. "Lidar remote sensing of the canopy structure and biophysical properties of Douglas-fir western hemlock forests." Remote Sensing of the Environment 70 (3): 339-361.

Mallet, C., and F. Bretar. 2009. "Full-waveform topographic lidar: state-of-the-art." ISPRS Journal of Photogrammetry and Remote Sensing 64 (1): 1-16.

Mücke, W., M. Hollaus, and N. Pfeifer. 2012. "Identification of dead trees using small footprint full-waveform airborne laser scanning data." Paper presented at SilviLaser 2012, the 12th International Conference on LiDAR Applications for Assessing Forest Ecosystems, Vancouver, BC, September 16-19.

Neuenschwander, A. 2012. "Mapping vegetation structure in a wooded savanna at Freeman Ranch, TX using airborne waveform LiDAR." Paper presented at SilviLaser 2012, the 12th International Conference on LiDAR Applications for Assessing Forest Ecosystems, Vancouver, BC, September 16-19.

Neuenschwander, A.L. 2008. "Evaluation of waveform deconvolution and decomposition retrieval algorithms for ICESat/GLAS data." Canadian Journal of Remote Sensing 34 (S2): S240-S246.

Neuenschwander, A.L., L. A. Magruder, and M. Tyler. 2009. "Landcover classification of small-footprint, full-waveform lidar data." Journal of Applied Remote Sensing 3 (1): 033544-033544.

Ni-Meister, W., D. L. Jupp, and R. Dubayah. 2001. "Modeling lidar waveforms in heterogeneous and discrete canopies." IEEE Transactions on Geoscience and Remote Sensing 39 (9): 1943-1958.

Pang, Y., M. Lefsky, G. Sun, and J. Ranson. 2011. “Impact of footprint diameter and off-nadir pointing on the precision of canopy height estimates from spaceborne lidar.” Remote Sensing of the Environment 115 (11): 2798-2809.

Peterson, B., K. Nelson, and B. Wylie. 2012. “Monitoring aboveground biomass in the Yukon River Basin using multi-scale LiDAR.” Paper presented at SilviLaser 2012, the 12th International Conference on LiDAR Applications for Assessing Forest Ecosystems Vancouver, BC, Sept. 16-19.

Reitberger, J., C. Schnörr, P. Krzystek, and U. Stilla. 2009. “3D segmentation of single trees exploiting full waveform LIDAR data.” ISPRS Journal of Photogrammetry and Remote Sensing 64 (6): 561-574.

Reitberger, J., P. Krzystek, and U. Stilla. 2008. “Analysis of full waveform LIDAR data for the classification of deciduous and coniferous trees.” International Journal of Remote Sensing 29 (5): 1407-1431.

Sarrazin, M.J.D., J. A. N. van Aardt, G. P. Asner, J. McGlinchy, D. W. Messinger, and J. Wu. 2012. “Fusing small-footprint waveform LiDAR and hyperspectral data for canopy-level species classification and herbaceous biomass modeling in savanna ecosystems.” Canadian Journal of Remote Sensing 37 (6): 653-665.

Sumnall, M.J., R.A. Hill, and S. A. Hinsley. 2012. “The estimation of forest inventory parameters from small-footprint waveform and discrete return airborne LiDAR data.” Paper presented at SilviLaser 2012, the 12th International Conference on LiDAR Applications for Assessing Forest Ecosystems Vancouver, BC, September 16-19.

Sun, G., K. J. Ranson, D. S. Kimes, J. B. Blair, and K. Kovacs. 2008. “Forest vertical structure from GLAS: An evaluation using LVIS and SRTM data.” Remote Sensing of the Environment 112 (1): 107-117.

The American Society for Photogrammetry & Remote Sensing. 2012. “LAS specification: version 1.3 – R11.” The Imaging & Geospatial Information Society.

van Leeuwen, M., and M. Nieuwenhuis. 2010. “Retrieval of forest structural parameters using LiDAR remote sensing.” European Journal of Forest Research 129 (4): 749-770.

Wu, J., J. A. N. van Aardt, J. McGlinchy, and G. P. Asner. 2012. “A Robust Signal Preprocessing Chain for Small-Footprint Waveform LiDAR.” IEEE Transactions on Geoscience and Remote Sensing 50 (8): 3242-3255.

Wu, J., J. A. van Aardt, G. P. Asner, T. Kennedy-Bowdoin, D. Knapp, B. F. Erasmus, R. Mathieu, K. Wessels, and I. P. Smit. 2009. “LiDAR Waveform-based woody and foliar biomass estimation in savanna environments.” Paper presented at Silvilaser 2009, the 9th International Conference on LiDAR Applications for Assessing Forest Ecosystems, College Station, TX, October 14-16.

Yang, W., W. Ni-Meister, and S. Lee. 2011. “Assessment of the impacts of surface topography, off-nadir pointing and vegetation structure on vegetation lidar waveforms using an extended geometric optical and radiative transfer model.” Remote Sensing of the Environment 115 (11): 2810-2822.

Yao, W., P. Krzystek, and M. Heurich. 2012. “A sensitivity analysis for a novel individual tree segmentation algorithm using 3D lidar point cloud data.” Paper presented at SilviLaser 2012, the 12th International Conference on LiDAR Applications for Assessing Forest Ecosystems, Vancouver, BC, September 16-19.

Table 1. Spatio-temporal metric values for the various waveforms related to hits located within the same vertical space. WF = Waveform (see Figure 4), HOME = Height of Median Energy, Vertical Distribution Ratio, NP = Number of Peaks, RWE = Return Waveform Energy.

| WF | HOME | VDR | NP | RWE |
|---|---|---|---|---|
| b | 41.2 | 0.02 | 1 | 403 |
| c | 41.2 | 0.00 | 4 | 292 |
| d | 40.2 | 0.04 | 3 | 431 |
| e | 17.1 | 0.59 | 1 | 526 |
| f | 17.7 | 0.58 | 1 | 485 |
| g | 30.8 | 0.27 | 3 | 280 |
| h | 35.9 | 0.15 | 6 | 308 |
| CV | 0.33 | 1.09 | 0.70 | 0.25 |

Figure 1. Returned intensity variation in relation to scanning angle. Mean ±standard deviation values are shown.

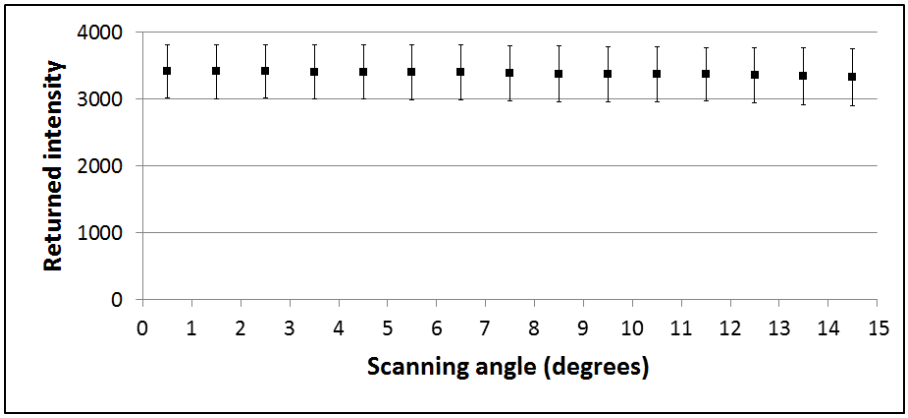

Figure 2. Histogram of LiDAR pulses relative to scanning angle.

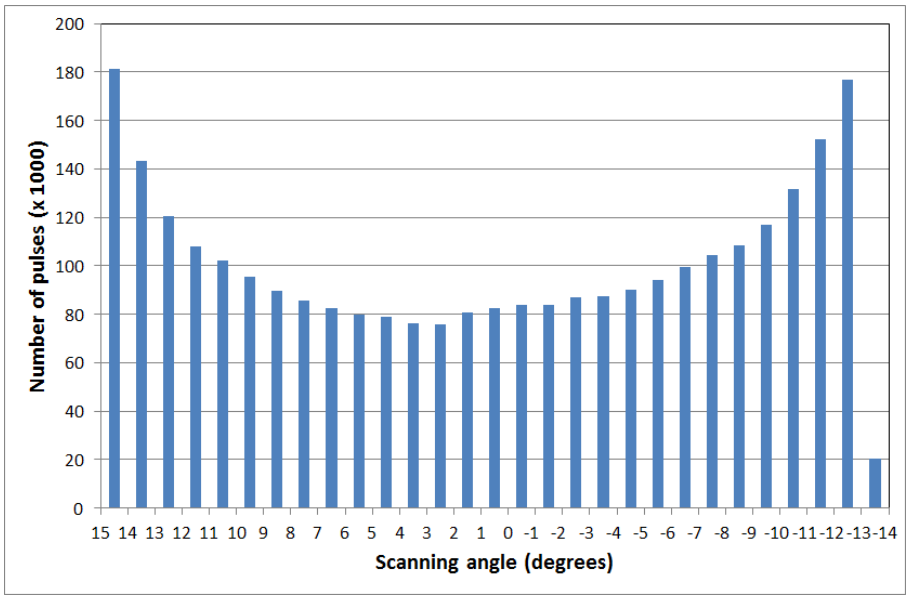

Figure 3. Horizontal displacement for off-nadir scanning angles computed per 1 m change in height increment.

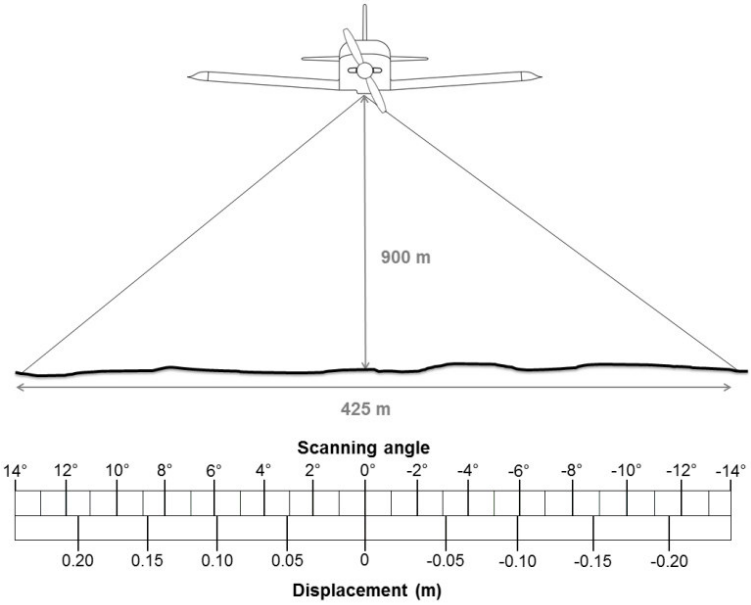

Figure 4. Pseudo-vertical waveform of an specific voxel column (a), and observed full-waveforms related to hits within the same vertical space (b, c, d, e, f, g, h).

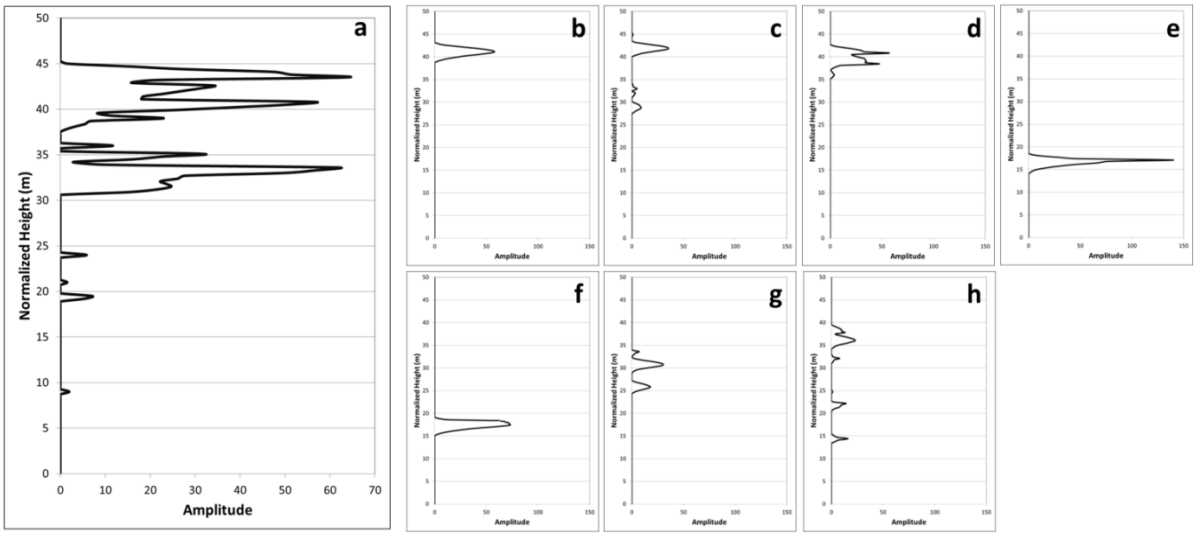

Figure 5. (a) Normalized digital surface model showing the height distribution of an example plot. (b) Graphical representation of a set spatio-temporal metrics characterizing the observed off-nadir full-waveforms (above) and the composite pseudo-vertical full-waveforms (below). The acronyms and abbreviations used are: HOME: height of median energy; RWE: return waveform energy; NP: number of peaks; and Rough.: roughness of outermost canopy.